Blindly Evaluating Stereoscopic Image Quality with Free-Energy Principle

Yucheng Zhu, Guangtao Zhai, Ke Gu, and Min Liu
Insti. of Image Commu. & Infor. Proce., Shanghai Jiao Tong University, Shanghai, China
Shanghai Key Laboratory of Digital Media Processing and Transmissions
{zyc420, zhaiguangtao, gukesjtuee, liumin_merry}@sjtu.edu.cn

***Abstract*—Three-dimensional (3D) imaging technology has been growingly prevalent in today's world. But objective quality assessment of 3D images is a challenging task. In this paper, we propose a blind metric to predict the perceptual quality of stereopairs within the concept of free energy. On the basis of a psychological measure, the free energy is a principle telling where supervises more and attracts human attention. We believe that the "surprise" can account for the binocular rivalry and thus be used to predict the quality of stereopairs. We first evaluate the quality of the monoscopic image, then introduce the computation process of binocular rivalry's results for deciding the relative importance of the left and right views, and finally infer the overall quality score. Our algorithm is tested on the symmetric LIVE3D-I and asymmetric LIVE3D-II databases. Experimental results confirm that the proposed blind 3D IQA technique, without distortion identification, is able to faithfully predict the visual quality of stereopairs.**

***Keywords*—Image quality assessment (IQA), binocular rivalry, free energy, stereoscopic, no-reference (NR), asymmetric.**

I. Introduction

Three-dimensional (3D) media services, which are becoming increasingly popular in today's world, are, to some extent, altering the way in which we entertain, communicate, and store information. The prevalence can be partly demonstrated by the number of 3D silver screens worldwide from 2006 to 2014. The number of screens in 2014, which is 22.3% higher than that of 2013 and is 251.6 times as much as that of 2006, reaches 64905. Apart from 3D movies, there is a glut of non-cinematic 3D content that is making its way to consumers, especially over wireless networks such as 3D on mobile devices, 3D TVs, 3D displays, 3D broadcast and some emerging wearable equipment [1]. However, the wireless transmission mode and the spotty displays imply the presence of types of distortions, which will be received by consumers and degrade the viewing experience. So we need systems to monitor, control and improve the visual quality of stereoscopic presentations. Image quality assessment (IQA), due to its capability of simulating human visual perception to image quality, is usually used to solve this problem.

Numerous approaches for 2D IQA have been proposed over the last several decades. In the current research of IQA, image quality metrics are usually classified into full-reference (FR) [2], [3], reduced-reference (RR) [4], [5], no-reference (NR) [6], [7] methods depending on the accessibility to the original reference points [8]. Some of them perform quite well in predicting the subject ratings on popular image quality databases [9], [10], [11].

Following the research of monoscopic image quality metrics, more and more objective 3D metrics have been developed. Compared with 3D subjective assessment methods, they are time-saving, convenient, and more practical for real-time image processing systems. We can classify the existing 3D IQA approaches into three categories: 1) [12], [13], [14], etc evaluate stereoscopic images using 2D IQA metrics; 2) [15], [16], etc measure stereoscopic images considering 3D perceptual properties; 3) [17], [18], [19], etc are NR/blind IQA approaches for stereoscopic images. In addition, several databases of 3D image sets as important tools in the research of 3D IQA have been proposed, such as LIVE 3D IQA Database including the Phase I dataset [1] and Phase II dataset [20], which make us convenient to analyze the performance of a variety of 3D quality metrics.

The additional dimension of 3D content brings about many important issues. First, the binocular rivalry may influence the perceived 3D quality [21]. Further, the depth sensation associated with depth quality, 2D quality, etc has a certain effect [22]. What's more, the incorrect stereography will degrade the experience of viewing a 3D image [23]. In this paper, we try to predict 3D perceptual quality by focusing on the two factors of all: the binocular rivalry and the quality of 2D binocular images. We propose a blind 3D IQA algorithm on the basis of 2D IQA NFERM [7] and resort to free-energy principle [24] to emulate the result of binocular rivalry. It is worth mentioning that Zhai *et al*. first apply the brain theory into IQA research in [4] and introduce a new approach based on free-energy principle. Some brain theories have been unified within the free-energy framework. In [24] Frison indicates that the uncertainty will be removed by human to infer the meaningful part from visual stimuli during the inference process of human brain. It is natural that there exists a gap between the real scene and the brain's prediction due to the fact that the internal generative model cannot be universal. It is the gap that makes human "surprise", and thus attracts attention. In other words, when images presented to two eyes are different, the image causing more surprise draws more attention. And we believe that the surprise can account for the binocular rivalry. In our algorithm, we use free-energy theory to predict the responses of human brain. On the basis of the responses, we generate the error map and compute the surprise. Finally we use spatial pooling strategy and get the blind 3D IQA algorithm.

The rest of this paper is organized as follows. Section II first presents the proposed IQA metric. In Section III, the effectiveness of our algorithm is proved by comparison of its experimental results with those obtained by existing relevant models. Finally, concluding remarks are given in Section IV.

II. Blind 3D Image Quality Assessment Via Free Energy Principle

Given an image signal I, the free-energy principle [24] suggests that the cognitive process is governed by an internal generative model $\mathcal{G}$ in the brain. Given different scenes or images, the model $\mathcal{G}$ will adapt itself through varying a parameter vector θ [4]. Then the "surprise" caused by image I can be computed by integrating the joint distribution $P(I, \theta|\mathcal{G})$ over the space of model parameter θ

$$-\log P(I|\mathcal{G}) \quad = \quad -\log \int P(I, \theta|\mathcal{G}) d\theta. \tag{1}$$

We can use an auxiliary posterior distribution $Q(\theta|I, \mathcal{G})$ to calculate the surprise of I in (1). Referring to [4], we can drop the latent model assumption $\mathcal{G}$ in our analysis for simplicity, since the behavior of the model can be characterized by parameter θ. By letting the auxiliary term into (1) and using Jensen's inequality we have

$$-\log P(I) \quad \leq \quad -\int Q(\theta|I) \log \frac{P(I, \theta)}{Q(\theta|I)} d\theta. \tag{2}$$

The right hand side of (2) is defined as the free energy:

$$F(I, \theta) \quad = \quad -\int Q(\theta|I) \log \frac{P(I, \theta)}{Q(\theta|I)} d\theta. \tag{3}$$

By noticing that $P(I, \theta) = P(\theta|I)P(I)$, we can write (3) into

$$\begin{aligned} F(I, \theta) &= \int Q(\theta|I) \log \frac{Q(\theta|I)}{P(\theta|I)P(I)} d\theta \\ &= -\log P(I) + \int Q(\theta|I) \log \frac{Q(\theta|I)}{P(\theta|I)} d\theta \\ &= E_Q[-\log P(I|\theta)] + KL\left(Q(\theta|I) \| P(\theta)\right). \end{aligned} \tag{4}$$

Here the term $KL\left(Q(\theta|I) \| P(\theta)\right)$ measures the distance between the recognition densities and the true prior of the model parameters. The term $E_Q[-\log P(I|\theta)]$ is the averaged entropy of predicting I.

We hope to compute the surprise. For operational amenability we can hypothesize the generative model $\mathcal{G}$ to be a 2D linear autoregressive (AR) model for its high description capability for natural images. The AR model is defined as

$$x_n \quad = \quad \boldsymbol{\chi}^k(x_n)\boldsymbol{\alpha} + \varepsilon_n \tag{5}$$

where x_n is the n_{th} pixel, $\boldsymbol{\chi}^k(x_n)$ is a row-vector that consists of k nearest neighbors of x_n, $\boldsymbol{\alpha} = (\alpha_1, \alpha_2, \alpha_3, ..., \alpha_k)^T$ is the vector of AR coefficients and the ε_n is the error term. Under the large sample condition, the free energy equals the total description length of image I. So we estimate the AR coefficients by minimizing the description length

$$\hat{\boldsymbol{\alpha}} \quad = \quad \arg\min_{\alpha}(-\log P(I|\boldsymbol{\alpha}) + \frac{k}{2}\log N) \tag{6}$$

where N is the data sample size. We fix the order and the training set size of the model and thus turn the comparison process into residual minimization

$$\hat{\boldsymbol{\alpha}} \quad = \quad \arg\min_{\alpha} ||x - \mathbf{X}\boldsymbol{\alpha}||_2 \tag{7}$$

where $x = (x_1, x_2, ..., x_N)^T$ and $\mathbf{X}(n, :) = \boldsymbol{\chi}^k(x_n)$. And the parameter can be solved as $\hat{\boldsymbol{\alpha}} = (\mathbf{X}^T\mathbf{X})^{-1}\mathbf{X}^T x$. In this case, the parameter θ of the model can be well described by $\hat{\boldsymbol{\alpha}}$.

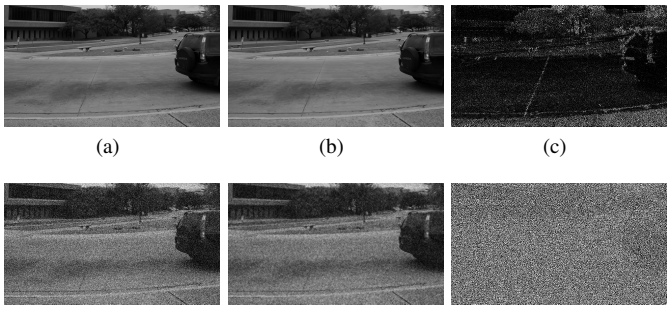

Fig. 1: Error map construction: (a) is of good quality, (d) is spoiled by white noise. (b) and (e) show the predicted images. (c) and (f) show the final computed error maps after scaling.

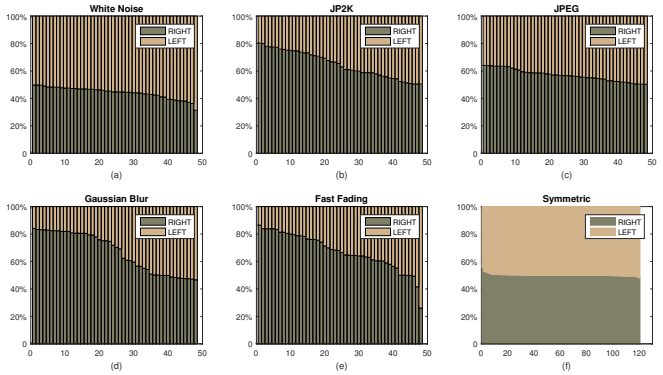

Fig. 2: Computed ratios of surprise: On Phase II dataset, the left-view images are of good quality or slightly spoiled, the right-view images are almost heavily spoiled. X-axis represents the number of images, y-axis represents the ratio of $R(E)$ between stereopairs, two colors of bar respectively represent left view and right view. (a) - (e) are statistical results of asymmetric stereopairs with different kinds of distortions. (f) is the result of symmetric stereopairs.

Next, we use the input image I in a point-wise manner to estimate the predicted version I_p via $\boldsymbol{\chi}^k(x_n) \cdot \hat{\boldsymbol{\alpha}}$. The point-wise error ε_n can then be pooled to get the error map $E(I)$ and entropy of the errors can also be computed as $R(E) = \sum -P(\varepsilon)\log P(\varepsilon)$ with $P(\varepsilon)$ being the probability distribution of the errors.

By above analysis, the linear AR model is used to approximate the generative model, thereby to predict an image that the HVS perceives from the outside stimulus. Then we compute the $R(E)$ from the predicted image which contributes to the surprise in human brain. We choose two images for analysis, one is the reference image from 3D LIVE database and the other is the spoiled version with white noise. Fig. 1.(a)-(f) show the predicted images and the scaled error maps. We intuitively deduce that the $R(E)$ of the image spoiled by white noise is larger because its error map seems wide-ranging. Experimental results prove our deduction, Fig. 2 gives the statistical results on Phase II dataset. The figure shows that when an asymmetric stereopair is spoiled by white noise, the worse image will cause more surprise. However other listed kinds of distortion lead to opposite results. Besides, the ratios of symmetrically distorted and asymmetrically white-noise stereopairs almost go

TABLE I: Comparison of 2D IQA Models: Pearson linear correlation coefficient (PLCC) against DMOS on the **Phase I** dataset. Italics indicates an NR (blind) algorithm.

Algorithm	Type	JP2K	JPEG	WN	BLUR	FF	All
PSNR	FR	0.788	0.208	0.926	0.916	0.711	0.835
SSIM [2]	FR	0.875	0.489	0.928	0.917	0.726	0.877
BRISQUE [6]	NR	*0.850*	*0.655*	*0.941*	*0.926*	*0.716*	*0.887*
NFERM [7]	NR	*0.896*	*0.669*	*0.903*	*0.924*	*0.811*	*0.893*
Our model	NR	*0.892*	*0.735*	*0.911*	*0.926*	*0.799*	***0.905***

TABLE II: Comparison of 3D IQA Models: Pearson linear correlation coefficient (PLCC) against DMOS on the **Phase I** dataset.

Algorithm	Type	JP2K	JPEG	WN	BLUR	FF	All
Benoit [12]	FR	0.940	0.641	0.925	0.949	0.747	0.903
Hewage [15]	RR	0.904	0.531	0.896	0.798	0.670	0.830
You [16]	FR	0.878	0.487	0.941	0.920	0.730	0.881
Gorley [26]	FR	0.485	0.312	0.796	0.853	0.365	0.451
Akhter [17]	NR	*0.906*	*0.729*	*0.905*	*0.618*	*0.660*	*0.427*
Our model	NR	*0.892*	*0.735*	*0.911*	*0.926*	*0.799*	***0.905***

halves, which implies the method by averaging the quality of stereopair predicted by 2D IQA algorithms can perform well on the two parts as shown in Table I-V.

Motivated by the fact that the receptive fields of the human visual cortex are localized in space [25] we further partition the distorted image into $M \times N$ patches. We calculate local entropy of error map on each block first. Then we apply them to our pooling strategy based on the idea that the spatial location that draws more attention deserves greater weight.

$$R^{'} = \Sigma_i \ \max[\ \frac{\xi \sigma_i}{\Sigma_i \ \sigma_i}\ ,\ \frac{R(E_i)}{\Sigma_i \ R(E_i)}\ ] \cdot R(E_i). \tag{8}$$

In (8) σ_i is the standard deviation of i_{th} block and $R(E_i)$ is entropy of local error map. There is a roughly linear relation between terms $\frac{\sigma_i}{\Sigma_i \ \sigma_i}$ and $\frac{R(E_i)}{\Sigma_i \ R(E_i)}$ according to observation of experimental results and we use parameter ξ and the $\max$ operator to improve the accuracy. We compute $R^{'}$ by three steps of partitioning distorted image, local computation to obtain $R(E_i)$ and σ_i, spatial pooling to obtain $R^{'}$. We use terms $w_l = R_l^{'}/(R_l^{'} + R_r^{'})$ and $w_r = R_r^{'}/(R_l^{'} + R_r^{'})$ as weights assigned for the left view and right view and thus compute the overall quality score by $s = w_l s_l + w_r s_r$.

We refer to the NFERM [7] as the 2D IQA algorithm in our model for the unification of free-energy principle and extract 23 features as NFERM does. Those features can be classified into three groups taking account of structural information, properties of HVS, and "naturalness" of images respectively. The obtained coefficients for 2D model are from training on the LIVE database and are not changed through the whole process. To save space we don't give detailed illustration here. Using two weights to linearly combine the two NFERM scores of the left and right views, we can derive the final prediction of our blind 3D IQA technique. The diagram of proposed model is shown in Fig. 3.

III. Experiments and Analysis

We use LIVE 3D Image Quality Database to validate the effectiveness of our method. This database was constructed in two phases. Phase I contains symmetrically distorted stimuli while Phase II has both symmetrically and asymmetrically distorted stimuli. Both phases used five types of distortions: compression using the JPEG and JPEG2000 compression

TABLE III: Comparison of 2D IQA Models: Pearson linear correlation coefficient (PLCC) against DMOS on the **Phase II** dataset. Italics indicates an NR (blind) algorithm.

Algorithm	Type	JP2K	JPEG	WN	BLUR	FF	All
PSNR	FR	0.501	0.378	0.855	0.727	0.439	0.471
SSIM [2]	FR	0.725	0.670	0.926	0.842	0.865	0.802
BRISQUE [6]	NR	*0.588*	*0.662*	*0.927*	*0.517*	*0.789*	*0.617*
NFERM [7]	NR	*0.685*	*0.504*	*0.740*	*0.923*	*0.832*	*0.724*
Our model	NR	*0.799*	*0.874*	*0.928*	*0.973*	*0.891*	***0.875***

TABLE IV: Comparison of 3D IQA Models: Pearson linear correlation coefficient (PLCC) against DMOS on the **Phase II** dataset.

Algorithm	Type	JP2K	JPEG	WN	BLUR	FF	All
Benoit [12]	FR	0.784	0.853	0.926	0.535	0.807	0.748
Hewage [15]	RR	0.664	0.734	0.891	0.450	0.746	0.558
You [16]	FR	0.905	0.830	0.912	0.784	0.915	0.800
Gorley [26]	FR	0.372	0.322	0.874	0.934	0.706	0.515
Akhter [17]	NR	*0.776*	*0.786*	*0.722*	*0.795*	*0.674*	*0.568*
Our model	NR	*0.799*	*0.874*	*0.928*	*0.973*	*0.891*	***0.875***

TABLE V: Break down of performance on symmetrically and asymmetrically distorted stimuli in the **Phase II** dataset. Spearman rank-order correlation coefficient (SROCC) numbers are reported.

Algorithm	Type	Symmetric	Asymmetric
PSNR	FR	0.776	0.587
SSIM [2]	FR	0.828	0.733
BRISQUE [6]	NR	*0.849*	*0.667*
NFERM [7]	NR	*0.773*	*0.670*
Benoit [12]	FR	0.860	0.671
You [16]	FR	**0.914**	0.701
Gorley [26]	FR	0.383	0.056
Hewage [15]	RR	0.656	0.496
Akhter [17]	NR	*0.420*	*0.517*
Our model	NR	*0.893*	***0.840***

standards, additive white Gaussian noise, Gaussian blur and a fast-fading model. Phase I has 20 pristine stereopairs and 365 distorted stereopairs, while Phase II has 8 pristine stereopairs and 360 distorted stereopairs. Table I-II for Phase I and Table III-V for Phase II are presented.

Pearson linear correlation coefficient (PLCC) and Spearman rank-order correlation coefficient (SROCC) are used to evaluate performance of our approach. PLCC can be considered as a measure of prediction accuracy, while SROCC measures the monotonicity by ignoring the relative distance between data. The higher SROCC and PLCC values indicate better performance in terms of correlation with human opinion.

We experimented on the Phase I dataset first to compare the performance of dealing with symmetrically distorted stereopairs. We compared the performance of our Blind 3D IQA algorithm with several 2D FR and NR IQA models: PSNR, SSIM [2], BRISQUE [6], NFERM [7]. For all 2D IQA algorithms, the predicted quality of a stereopair is taken to be the average quality predicted from the left and right views. 2D IQA algorithms perform well on this symmetric dataset as illustrated in previous section. Our method achieves high performance and performs as well as NFERM as shown in Table I. We also studied the relevant performance of 3D IQA algorithms and our algorithm outperforms most of them as shown in Table II. Although there is little or no binocular rivalry from the distortions present in the stimuli in Phase I dataset and there is no prior knowledge to reference images

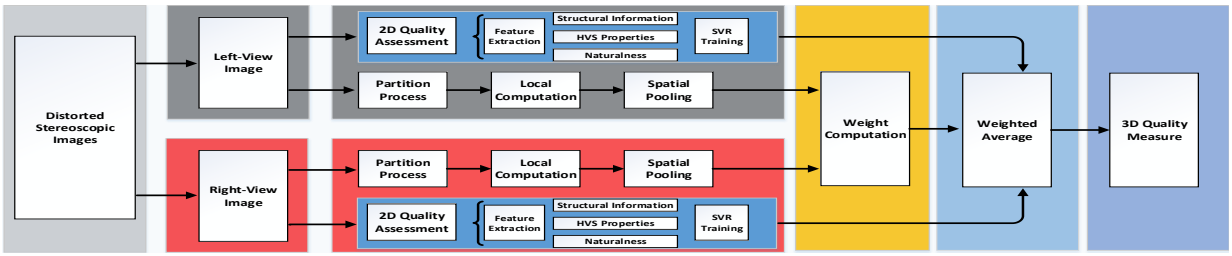

Fig. 3: Diagram of our proposed 3D IQA algorithm. Light-gray portion delivers the distorted stereoscopic images, deep-gray portion disposes left view, red portion disposes right view, yellow part calculates the weight, light-blue part calculates averaged scores and finally deep-blue part gets the result.

and distortion types, our algorithm matches those listed FR algorithms in most aspects.

The Phase II dataset has both symmetrically and asymmetrically distorted stimuli. Tables III-V show the results against the mixed dataset. 2D IQA algorithms perform well on the white-noise dataset as illustrated in previous section. Our algorithm delivers the best performance compared against most other algorithms. Besides, we further compare our method with existing 3D IQA metrics. Among individual distortion types, our model performes either the best or at parity with the best for all distortion types. Table V shows the high performance of our model compared against FR PSNR, SSIM [2], Benoit [12], You [16], Gorley [26], RR Hewage [15], NR BRISQUE [6], NFERM [7], and Akhter [17] on the completely asymmetrically distorted stimuli as we expect.

IV. Conclusion

In this paper, we propose a blind 3D image quality assessment algorithm based on free-energy principle. The resulting algorithm utilizes binocular rivalry based on the brain theory and properties of HVS and features previously proposed for 2D NR algorithms. Under both symmetrically and asymmetrically distorted conditions, our algorithm outperforms NR IQA models and delivers competitive performance relative to FR IQA models on the 3D LIVE Database.

Acknowledgment

This work was supported in part by the National Science Foundation of China under Grants 61422112, 61371146, 61521062, 61527804, the Foundation for the Author of National Excellent Doctoral Dissertation of China under Grant 201339 and National High-tech R&D Program of China under Grant 2015AA015905.

References

[1] A. K. Moorthy, C.-C. Su, A. Mittal, and A. C. Bovik, "Subjective evaluation of stereoscopic image quality," *Signal Processing: Image Communication*, vol. 28, no. 8, pp. 870–883, 2013.

[2] Z. Wang, A. C. Bovik, H. R. Sheikh, and E. P. Simoncelli, "Image quality assessment: from error visibility to structural similarity," *Image Processing, IEEE Transactions on*, vol. 13, no. 4, pp. 600–612, 2004.

[3] K. Gu, G. Zhai, X. Yang, and W. Zhang, "An efficient color image quality metric with local-tuned-global model," *in Proc. IEEE Int. Conf. Image Process.*, pp. 506-510, Oct. 2014.

[4] G. Zhai, X. Wu, X. Yang, W. Lin, and W. Zhang, "A psychovisual quality metric in free-energy principle," *Image Processing, IEEE Transactions on*, vol. 21, no. 1, pp. 41–52, 2012.

[5] K. Gu, G. Zhai, X. Yang, and W. Zhang, "A new reduced-reference image quality assessment using structural degradation model," *in Proc. IEEE Int. Symp. Circuits and Syst.*, pp. 1095-1098, May 2013.

[6] A. Mittal, A. K. Moorthy, and A. C. Bovik, "No-reference image quality assessment in the spatial domain," *IEEE Trans. Image Process.*, vol. 21, no. 12, pp. 4695-4708, Dec. 2012.

[7] K. Gu, G. Zhai, X. Yang, and W. Zhang, "Using free energy principle for blind image quality assessment," *Multimedia, IEEE Transactions on*, vol. 17, no. 1, pp. 50–63, 2015.

[8] W. Lin and C.-C. J. Kuo, "Perceptual visual quality metrics: A survey," *Journal of Visual Communication and Image Representation*, vol. 22, no. 4, pp. 297–312, 2011.

[9] H. R. Sheikh, Z. Wang, L. Cormack, and A. C. Bovik, "LIVE image quality assessment Database Release 2," [Online]. Available: http://live.ece.utexas.edu/research/quality

[10] N. Ponomarenko, O. Ieremeiev, V. Lukin, K. Egiazarian, L. Jin, J. Astola, B. Vozel, K. Chehdi, M. Carli, F. Battisti *et al.*, "Color image database tid2013: Peculiarities and preliminary results," in *Visual Information Processing (EUVIP), 2013 4th European Workshop on*. IEEE, 2013, pp. 106–111.

[11] K. Gu, G. Zhai, W. Lin, and M. Liu, "The analysis of image contrast: From quality assessment to automatic enhancement," *IEEE Trans. Cybernetics*, vol. 45, 2015.

[12] A. Benoit, P. Le Callet, P. Campisi, and R. Cousseau, "Quality assessment of stereoscopic images," *EURASIP journal on image and video processing*, vol. 2008, pp. Article–ID, 2008.

[13] J. Wang, A. Rehman, K. Zeng, S. Wang and Z. Wang, "Quality prediction of asymmetrically distorted stereoscopic 3D images," *IEEE Trans. Image Process.*, vol. 24, no. 11, pp. 3400-3414, Nov. 2015.

[14] Jiheng Wang, Kai Zeng, and Zhou Wang, "Quality prediction of asymmetrically distorted stereoscopic images from single views," in *Multimedia and Expo (ICME), 2014 IEEE International Conference on*. IEEE, 2014, pp. 1–6.

[15] C. T. Hewage and M. G. Martini, "Reduced-reference quality metric for 3d depth map transmission," in *3DTV-Conference: The True Vision-Capture, Transmission and Display of 3D Video (3DTV-CON), 2010*. IEEE, 2010, pp. 1–4.

[16] J. You, L. Xing, A. Perkis, and X. Wang, "Perceptual quality assessment for stereoscopic images based on 2d image quality metrics and disparity analysis," in *Proc. of International Workshop on Video Processing and Quality Metrics for Consumer Electronics, Scottsdale, AZ, USA*, 2010.

[17] R. Akhter, Z. P. Sazzad, Y. Horita, and J. Baltes, "No-reference stereoscopic image quality assessment," in *IS&T/SPIE Electronic Imaging*. International Society for Optics and Photonics, 2010, pp. 75 240T–75 240T.

[18] K. Gu, G. Zhai, X. Yang, and W. Zhang, "No-reference stereoscopic iqa approach: From nonlinear effect to parallax compensation," *Journal of Electrical and Computer Engineering*, vol. 2012, 2012.

[19] F. Shao, W. Lin, S. Wang, G. Jiang, and M. Yu, "Blind image quality assessment for stereoscopic images using binocular guided quality lookup and visual codebook."

[20] M.-J. Chen, L. K. Cormack, and A. C. Bovik, "No-reference quality assessment of natural stereopairs," *Image Processing, IEEE Transactions on*, vol. 22, no. 9, pp. 3379–3391, 2013.

[21] P. Seuntiens, L. Meesters, and W. Ijsselsteijn, "Perceived quality of compressed stereoscopic images: Effects of symmetric and asymmetric jpeg coding and camera separation," *ACM Transactions on Applied Perception (TAP)*, vol. 3, no. 2, pp. 95–109, 2006.

[22] W. Chen, J. Fournier, M. Barkowsky, and P. Le Callet, "Quality of experience model for 3dtv," in *IS&T/SPIE Electronic Imaging*. International Society for Optics and Photonics, 2012, pp. 82 881P–82 881P.

[23] M. Lambooij, M. Fortuin, I. Heynderickx, and W. IJsselsteijn, "Visual discomfort and visual fatigue of stereoscopic displays: a review," *Journal of Imaging Science and Technology*, vol. 53, no. 3, pp. 30 201–1, 2009.

[24] K. Friston, "The free-energy principle: a unified brain theory?" *Nature Reviews Neuroscience*, vol. 11, no. 2, pp. 127–138, 2010.

[25] D. H. Hubel and T. N. Wiesel, "Receptive fields and functional architecture of monkey striate cortex," *The Journal of physiology*, vol. 195, no. 1, pp. 215–243, 1968.

[26] P. Gorley and N. Holliman, "Stereoscopic image quality metrics and compression," in *Electronic Imaging 2008*. International Society for Optics and Photonics, 2008, pp. 680 305–680 305.